Title: Effects of sodium arsenite on neurite outgrowth and glutamate AMPA receptor expression in mouse cortical neurons.
Authors: Maekawa F, Tsuboi T, Oya M, Aung KH, Tsukahara S, Pellerin L, Nohara K
Journal: Neurotoxicology
Year: 2013 Jul
Volume: 37
Pages: 197-206
DOI: 10.1016/j.neuro.2013.05.006

Effects of sodium arsenite on neurite outgrowth and glutamate AMPA receptor expression in mouse cortical neurons

Fumihiko Maekawa[1], Takashi Tsuboi[2], Kyaw Htet Aung[3], Shinji Tsukahara[3], Luc Pellerin[4], Keiko Nohara[1,5]

1. Center for Environmental Health Sciences, National Institute for Environmental Studies, Tsukuba 305-8506, Japan
2. Department of Life Sciences, Graduate School of Arts and Sciences, The University of Tokyo, 3-8-1 Komaba, Tokyo 153-8902, Japan.
3. Division of Life Science, Graduate School of Science and Engineering, Saitama University, Sakura-ku, Saitama City, Saitama 338-8570, Japan
4. Department of Physiology, University of Lausanne, Lausanne, 7 Rue du Bugnon, CH-1005 Lausanne, Switzerland.
5. Graduate School of Life and Environmental Sciences, University of Tsukuba, Tsukuba 305-8577, Japan

*Correspondence to Dr. Fumihiko Maekawa (fmaekawa@nies.go.jp)
Center for Environmental Health Sciences, National Institute for Environmental Studies, Tsukuba 305-8506, Japan

Abstract

There has been broad concern that arsenic in the environment exerts neurotoxicity. To determine the mechanism by which arsenic disrupts the neuronal development, primary cultured neurons obtained from the cerebral cortex of mouse embryos were exposed to sodium arsenite ($NaAsO_2$) at concentrations between 0 and 2 μM from day 2 to 4 *in vitro* and cell survival, neurite outgrowth and expression of glutamate AMPA receptor subunits were assessed at day 4 *in vitro*. Cell survival was significantly decreased by exposure to the 2 μM $NaAsO_2$ concentration, whereas the 0.5 μM of $NaAsO_2$ increased cell survival instead. The assessment of neurite outgrowth showed that total neurite length was significantly suppressed by 1 μM and 2 μM $NaAsO_2$, indicating that the lower concentration of $NaAsO_2$ impairs neuritogenesis before inducing cell death. Immunoblot analysis of AMPA receptor subunit expression showed that the protein level of GluA1, a specific subunit of the AMPA receptor, was significantly decreased by 1 μM and 2 μM $NaAsO_2$. When immunocytochemistry was used to confirm this effect by staining for GluA1 expression in neuropeptide Y neurons, most of which contain GluA1, GluA1 expression in neuropeptide Y neurons was found to be significantly suppressed by 1 μM and 2 μM $NaAsO_2$ but to be increased at the 0.5 μM concentration. Finally, to determine whether neurons could be rescued from the $NaAsO_2$-induced impairment of neuritogenesis by compensatory overexpression of GluA1, we used primary cultures of neurons transfected with a plasmid vector to overexpress GluA1, and the results showed that GluA1 overexpression protected against the deleterious effects of $NaAsO_2$ on neurite outgrowth. These results suggest that, 1) the toxic concentrations of $NaAsO_2$ in regard to cell survival, neurite outgrowth and GluA1 expression differ, 2) the $NaAsO_2$ concentration that induces neurite suppression is lower than the concentration that induces cell death and is almost the same as the concentration that suppresses GluA1 expression, and 3) the suppression of GluA1 expression by $NaAsO_2$ is at least partly responsible for neurite suppression induced by $NaAsO_2$.

Key words: Arsenic, Neuron, Neurite, Glutamate, GluA1

1. Introduction

The developing brain is vulnerable to toxic chemical compounds during gestation and early childhood, and exposure to them permanently affects brain functions (Costa et al., 2004; Grandjean and Landrigan, 2006). Heavy metals and persistent organic pollutants have been shown to be toxic to the developing brain epidemiologically and empirically (Winneke, 2011). Two heavy metals, inorganic lead and methylmercury are notorious causative agents that are responsible for the increased prevalence of mental retardation, cerebral palsy, autism, and attention-deficit hyperactivity disorder (ADHD) in children (Goulet et al., 2003; Costa et al., 2004; Farina et al., 2011; Winneke, 2011). Another metal, arsenic may also have neurotoxic effects on development. Follow-up studies of the victims of arsenic poisoning in the Morinaga milk incident in Japan have shown that the oral exposure to arsenic during infancy increases the prevalence of brain disorders, including mental retardation and epilepsy (Dakeishi et al. 2006). Additional evidence of the arsenic neurotoxicity was obtained in an epidemiological study of Mexican children living near a smelter demonstrated an inverse correlation between the children's urinary arsenic levels and their verbal intelligence quotients. (Calderón J et al., 2001). Epidemiological studies from Bangladesh, China and Taiwan have shown that chronic exposure to drinking water containing arsenic decreased the cognitive performance of children (Wang et al., 2007; Hamadani et al., 2011; Wasserman et al., 2004, 2007; Tsai et al., 2003), suggesting that arsenic has toxic effects on the central nervous system not only in the form of an industrial pollutant but also as an environmental contaminant of drinking water and food.

Empirical studies have been performed on experimental animals to determine how arsenic exposure impairs normal brain development. Rats and mice exposed to arsenic during gestation and early childhood exhibit behavioral deficits such as changes in locomotor activity, learning, memory, depression-like behavior and neuromotor reflex (Rodríguez et al., 2002, Xi et al., 2009, Martinez-Finley et al. 2009). The behavioral changes caused by arsenic seem to be accompanied by neurochemical abnormalities and loss of nerve fibers (Nagaraja and Desiraju, 1993; Martinez et al. 2008; Ríos et al., 2009). The inhibitory effects of arsenic on neuritogenesis have been monitored in *in vitro* experiments, and the results have been consistent with the results observed in animals *in vivo*. Studies conducted on immortalized cell lines have shown that arsenic impairs neurite outgrowth and complexity (Frankel et al., 2009). Arsenic is known to exert its neurotoxic effects by inducing apoptotic cell death as well as the inhibition of neuritogenesis (Koike-Kuroda et al., 2010). We recently reported finding that neurite elongation in the Neuro2A cell line was suppressed by sodium arsenite at a lower concentration than the concentration that induced

apoptosis (Aung et al., 2013). Thus, neuritogenesis would seem to be more sensitive to arsenic toxicity than cell viability is. Arsenic may exert its toxic effect through several different mechanisms, including at least the different mechanisms that are responsible for the suppression of neurite growth and for the induction of apoptosis, but the mechanisms are not completely understood.

Glutamate transmission plays essential roles in a variety of brain functions and in the development. AMPA receptors, a major subtype of glutamate receptors, are composed of four types of different subunits, i.e., GluA1, 2, 3 and 4, and play a critical role in excitatory glutamate transmission (Kumar and Mayer, 2012). AMPA receptors are also involved in the formation of neuronal networks and connectivity. Pharmacological potentiation of AMPA receptors and overexpression of either AMPA receptor subunit GluA1 or GluA2 by transient transfection promotes neurite outgrowth (Voss et al., 2007; Prithviraj et al., 2008; Chen et al., 2009). These results suggest that modifications of AMPA receptor subunit expression and subsequent increases in excitability due to enhanced glutamate transmission are closely related to the regulation of neuritogenesis.

In the present study, we investigated the effects of arsenic on AMPA receptors in primary cultures of mouse cortical neurons to determine the mechanism by which arsenic exposure suppresses neuritogenesis. Immunoblot and immunocytochemistry analyses showed that arsenic suppressed the level of GluA1 expression in parallel with the suppression of neurite outgrowth. We also transfected GluA1 into primary neurons with plasmid vectors to determine whether overexpression of AMPA receptors would rescue the neurite outgrowth suppressed by arsenic.

2. Materials and Methods

2.1 Mice

Male and female C57BL/6J mice were purchased from CLEA Japan (Tokyo, Japan) and were bred in National Institute for Environmental Studies. They were acclimatized to the environment for about 1 week prior to use. Throughout the experiment, animals were maintained in a controlled environment at a temperature of 24 ± 1 ^{o}C and humidity of 50 ± 10% and under a 12/12 h light/dark cycle (light, ZT0–12; dark, ZT12–24). Food (CE-2, CLEA) and water were available *ad libitum* unless otherwise indicated. Adult males and females were kept in couples to obtain pregnant females. Vaginal plug was checked each day to estimate the gestational age.

For the experiment focusing on neuropeptide Y (NPY) neurons, NPY-hrGFP transgenic mice produced by Prof. Bradford B. Lowell (Beth Israel Deaconess Medical Center) were purchased from the Jackson Laboratory (B6.FVB-Tg(Npy-hrGFP)1Lowl/J, Stock#006417, Bar Harbor, ME) (van den Pol et al., 2009). Adult males and females were genotyped by multiplex PCR of tail-derived DNA using the following three different primers: TAT GTG GAC GGG GCA GAA GAT CCA GG, CCC AGC TCA CAT ATT TAT CTA GAG, and GGT GCG GTT GCC GTA CTG GA. The PCR was performed using KOD dash (Toyobo, Tokyo, Japan) according to the manufacturer's instruction. The PCR reactions were performed using the following cycle conditions: 1) 94 °C for 3 min, 2) 35 cycles of 94 °C for 30 s, 58.5 °C for 5 s, and 74 °C for 30 s, and 3) 74 °C for 7 min. PCR products were subjected to electrophoresis on a 1.5 % agarose gel and the insertion of transgene was determined by the appearance of band sizes (transgene, 400 bp, and internal positive control, 500 bp). For culture of primary NPY-hrGFP neurons, the brain at embryonic day 17 was obtained and the green fluorescence in the cerebral cortex observed with either IX70 fluorescence microscope (Olympus, Tokyo, Japan) or BioRevo BZ-9000 (Keyence, Osaka, Japan).

2.2 Ethics Statement

Mice were handled in a humane manner in accordance with the National Institute for Environmental Studies guidelines.

2.3 Primary culture of neurons and transfection of plasmids

Primary cultures of mouse cortical neurons were prepared following the method described previously (Chenal and Pellerin, 2007) with slight modifications. Briefly, the pregnant mouse at embryonic day 17 was sacrificed by decapitation and the cerebral cortices of embryos were collected under dissection microscope. The cortices were washed with 10 mM HEPES-buffered Krebs-Ringer bicarbonate buffer (HKRB) containing 10 mM glucose. They were incubated in HKRB supplemented with 20 U/ml papain (Sigma Chemical Co., St. Louis, MO), 0.015 mg/ml deoxyribonuclease (Sigma), 0.75 mg/ml bovine serum albumin (Sigma) and 1 mM cysteine (Sigma) for 10 min at 37 °C in a shaking water bath, followed by gentle mechanical trituration. The subsequent cell suspension was centrifuged at 100 × g for 5 min and the cell pellet collected. In the case that transfection of plasmids was required, we used the Amaxa Nucleofector with mouse neuron nucleofector® kit (#VPG-1001, Lonza, Basel, Switzerland) following manufacturer's instruction. For tracing neurites, we used the pmStrawberry plasmid expressing

red fluorescent protein mStrawberry under the control of CMV promoter (Maekawa et al. 2009) in Fig. 1 B-I, Fig. 4, and Supplementary Fig.1. For overexpressions of GluA1 and 2, we used pGFP-GluA1 expressing GFP-fused GluA1 under the control of CMV promoter (kindly provided by Dr. Jeremy M. Henley, University of Bristol) and pVenus-GluA2 expressing GluA2-fused with Venus, a GFP variant, under the control of CMV promoter. Correct band sizes and surface expressions of fused proteins in primary cultures of neurons have been already determined previously (Perestenko and Henley, 2003; Maekawa et al., 2009). We used pEGFP (Clontech, Takara, Japan) expressing GFP as a control instead of pGFP-GluA1 and pVenus-GluA2. Cells undergoing or not transfection were resuspended in Neurobasal medium (Invitrogen, Carlsbad, CA) containing B-27 supplement (50×, Invitrogen), 0.5 mM L-glutamine (Invitrogen) and antibiotics (Pen/Strep, #15140-148, 100×, Invitrogen). Cells were seeded onto poly-L-ornithine (15 mg/L)-precoated coverslips (12 mm, Matsunami glass, Osaka, Japan) in 24 wells cell culture plates (Falcon, Becton Dickinson AG, Basel, Switzerland). Sodium arsenite ($NaAsO_2$) was added on the 2nd day *in vitro* (DIV2) and maintained up to DIV4 at different concentrations.

2.4 Cell survival assay

The effect of $NaAsO_2$ on cell survival of neurons was determined using a colorimetric assay based on the reduction of tetrazolium salt to formazan by mitochondrial dehydrogenase activity. Ten microliters of Tetrazolium reagent WST-1 (Roche, Switzerland) was then reacted with the cells at DIV4 for 1 h at 37 °C, and absorbance at 450 nm was then measured using a reference wavelength of 650 nm. The absorbance at 650 nm was subtracted from the absorbance at 450 nm, and this value was then expressed as a percentage of the value obtained for the neurons without $NaAsO_2$ exposure, whose viability was set at 100%.

2.5 Quantification of neurite outgrowth

At DIV4, cells were fixed with ice-cold 4% paraformaldehyde-phosphate buffered saline (PBS) for 30 min and washed with PBS. Coverslips were mounted with Vectashield Hard set with DAPI (H-1500, Vector Laboratories, Burlingame, CA). Images were taken with a Leica TCS SP5 AOBS filter free spectral confocal microscope (Leica Microsystems GmbH, Wetzlar, Germany). In Fig. 1 B-I, Fig. 4 and Supplementary Fig. 1, to trace neurites, the fluorescence of pmStrawberry was detected according to a previous report (Maekawa et al, 2009). Concerning the NPY-hrGFP neurons in Fig. 3 D-H, the fluorescence of hrGFP was detected following the setting of GFP (Maekawa et al, 2009). Full optical sections of cells were made by capturing Z-series with one

micrometer steps. The integrated image constructed from optical sections in order to define the details of neurites was made with Leica Application Suite-Advanced Fluorescence (LAS-AF, Version 1.8.2 build 1465, Leica). The images of either red or green channel from the integrated image were extracted to visualize either pmStrawberry or hrGFP, respectively, and was converted to gray scale to further assessment. The total length of neurites and the number of branches were examined by using the software NeuronJ (Meijering et al., 2004) which is a plug-in of ImageJ (NIH, Bethesda, MD). Neurites were categorized as "primary", which are neurites directly extending from cell body or "secondary and higher order", which are all neurites except "primary". The number of branches was counted following this categorization. For representative presentations in figures, the images inverted black with white were used for legibility.

2.6 Glutamate assay

To detect glutamate in culture medium, the glutamate research ELISA kit (#BA E-2300, LDN, Nordhorn, Germany) was used following manufacturer's instruction. Simultaneously, the amount of proteins in each culture well was determined with a BCA protein assay kit (Thermo Fisher Scientific, Yokohama, Japan) and glutamate levels corrected for protein level in each well.

2.7 Western blotting

Western blotting was carried out as described previously (Maekawa et al. 2009) with a minor modification. Briefly, cells were lysed in 0.5% Triton X-100 lysis buffer (50mM Tris-HCl, 150 mM NaCl, 5mM EDTA) containing proteinase inhibitors (1.9 mg/ml aprotinin, 10 mg/ml leupeptin, 100 mM sodium orthovanadate and 200 mM phenylmethylsulfonyl fluoride). The protein concentration of lysate was determined with a BCA protein assay kit and the value was used for equilibrating the protein level of each lane for SDS-PAGE. After boiling with SDS sample buffer (50mM Tris-HCl pH 6.8, 2% SDS, 10% glycerol, 100mM DTT, 0.001% bromphenol blue), the samples were subjected to SDS-PAGE and then transferred to PVDF membranes (Hybond-P, Thermo Fisher Scientific). The membranes were blocked by 1% casein-PBS for 1 hr and allowed to react with anti-GluA1 (1:1,000, AB1504, Millipore), anti-GluA2/3 (1:1,000, AB1506, Millipore), and anti-GluA4 (1:1,000, AB1508, Millipore), and anti-β-actin (1:5,000, Sigma-Aldrich) overnight at 4 °C, washed, and then allowed to react with horseradish peroxidase-conjugated secondary antibody (anti-rabbit IgG or anti-mouse IgG1) for 1 hr at room temperature. After washing, membranes were developed using the ECL Plus Western

Blotting Detection System (Thermo Fisher Scientific). Band density of each well was determined with ImageJ.

2.8 Immunocytochemistry and assessment of relative intensity of fluorescence

After fixating with ice-cold 4% paraformaldehyde-PBS and rinsing in PBS, cells were incubated with 1% casein-PBS for 1 hr at room temperature in order to block non-specific binding of antibody. Next, cells were incubated with rabbit anti-GluA1 (1:100), anti-GluA2/3 (1:100), and anti-GluA4 (1:100) in 1% casein-PBS for 24 hrs. After further washing with PBS, cells were incubated with AlexaFluor 594-labeled donkey anti-rabbit IgG (1:200, A21207, Invitrogen) for 2 hrs at 37 °C. After washing again with PBS, cells were examined with confocal microscope. The number of GluA1-positive neurons among NPY-hrGFP neurons was manually counted by using the integrated images of neurons without treatment with $NaAsO_2$. Relative intensity of GluA1 immunofluorescence was calculated in the area delineating the cell body of NPY-hrGFP neurons with or without treatment with $NaAsO_2$ by using LAS-AF.

2.9 Statistical analyses

Data are expressed as mean ± S.E.M. Replicates are indicated in parentheses. All data except Fig. 2E were analyzed by one-way ANOVA followed by Fisher's post-hoc least significant difference using R (The R Foundation for Statistical Computing, Vienna, Austria). Data in Fig. 2E were analyzed by Student's t-test with Microsoft Excel 2008 for Mac (Microsoft, Redmond, WA). Differences were considered significant for $p< 0.05$.

3. Results

3.1 Effect of $NaAsO_2$ on cell viability and neurite outgrowth

To determine the concentrations of $NaAsO_2$ that affect the survival of primary cultured neurons, we exposed them to $NaAsO_2$ concentrations of 0, 0.125, 0.25, 0.5, 1, and 2 μM from DIV2 to 4. As shown with the cell survival assay using WST-1 on DIV4 neurons, $NaAsO_2$ significantly reduced cell viability at the 2 μM concentration (Fig. 1A). However, no significant decrease in cell viability was observed at concentrations up to 1 μM (Fig. 1A). In contrast to the effect of the 2 μM concentration of $NaAsO_2$, the 0.5 μM concentration significantly increased the survival of primary neurons and the tendency to increase cell survival was also found at the 0.125 μM and 0.25 μM concentrations.

Analysis of the computer-assisted neurite tracings showed a significant reduction in total neurite

length per cell at the 1 μM and 2 μM concentrations of $NaAsO_2$ (Fig. 1F), and the degree of the reduction was greater at 2 μM (Fig. 1F). At 0.5 μM $NaAsO_2$ tended to increase total neurite length, but the difference between the effects of the 0 μM and 0.5 μM concentrations was not significant.

We also counted the number of total, primary, and secondary and higher order branches per cell. Although total number of branches tended to decrease as the concentration increased (1.0 μM vs 0 and 0.5 μM, p=0.09), there were no significant differences between the effects of the different concentrations on total number of branches or on the number of primary branches (Fig. 1G and H). The number of secondary and higher order branches in the group exposed to 1 μM or 2 μM $NaAsO_2$ were smaller than they were in the control group, but differences were not significant (Fig. 1I).

3.2 Effect of $NaAsO_2$ on extracellular glutamate levels and on the AMPA receptor expression

Since excitotoxicity induced by increases in extracellular glutamate levels is known to be involved in neurodegenerative diseases (Lau and Tymianski, 2010), we therefore suspected that $NaAsO_2$ elicits excitotoxicity by increasing extracellular glutamate levels. Extracellular glutamate levels were measured by collecting the culture medium of primary neurons that had been exposed to $NaAsO_2$ at concentrations of 0, 0.125, 0.25, 0.5, and 1 μM from DIV2 to 4 (Fig. 2A). However, no significant differences in glutamate levels were detected, suggesting that $NaAsO_2$ does not affect glutamate release by primary cultured cortical neurons. Next, we performed an immunoblot analysis to assess the levels of expression of AMPA receptor subunits. Cultured neurons were exposed to $NaAsO_2$ at concentrations of 0, 0.5, 1, and 2 μM from DIV2 to DIV4, and cell lysates were obtained at DIV4. Immunoblotting with anti-GluA1 antibody showed decreased expression of GluA1 in neurons exposed to 1 μM or 2 μM $NaAsO_2$ in comparison with neurons exposed to the 0 μM and 0.5 μM concentrations (Fig. 2B), but there were no significant difference in β-actin protein levels (Fig. 2B). Quantification of the GluA1/β-actin intensity ratio with the ImageJ software program revealed that exposure to $NaAsO_2$ at 1 μM or 2 μM significantly reduced GluA1 expression (Fig. 2C). As far as other AMPA receptor subunits are concerned, a comparison between neurons exposed to $NaAsO_2$ at concentrations of 0 μM and 1 μM was performed (Fig. 2D). In this experiment, we first confirmed the decreased GluA1 expression by the exposure to 1 μM $NaAsO_2$. Immunoblotting with anti-GluA2/3 and anti-GluA4 antibodies revealed no changes in GluA2/3 and GluA4 levels as a result of exposure to 1 μM $NaAsO_2$, suggesting that $NaAsO_2$ affects the expression of glutamate AMPA receptors in a

subunit-specific manner. Since we previously showed that $NaAsO_2$ has no significant effect on the mRNA levels of microtubule associated protein-2 (MAP2) and β-actin (Aung et al., 2013), we measured the protein levels of MAP2 and β-actin as negative controls in this study. As expected, there was no difference in their expression according to whether the cells had been exposed to 1 μM $NaAsO_2$ or not (Fig. 2D). Quantification of band density confirmed that exposure to 1 μM $NaAsO_2$ significantly reduces of GluA1 expression but does not reduce expression of any of the other subunits (Fig. 2E).

3.3 Effect of $NaAsO_2$ on GluA1 expression in primary cultured NPY-hrGFP neurons

To confirm the results of the immunoblot analyses showing that $NaAsO_2$ suppresses the GluA1 level by a different approach, we used primary cultures prepared from transgenic mice that express a humanized *Renilla* green fluorescence protein under the control of a neuropeptide Y gene promoter (NPY-hrGFP). The cerebral cortex emitting green fluorescence could be observed in the macroview of the mouse brain at embryonic day 17 by using BioRevo BZ-9000 (Fig. 3A). We easily identified NPY-hrGFP neurons in primary cultures of cortical neurons, because their cell bodies and neurites emitted green fluorescence (Fig. 3B). Immunofluorescence staining with anti-GluA1 antibody revealed that at DIV4 98.5% of the NPY-hrGFP neurons were GluA1-positive under our culture conditions (Fig. 3B and 3C). Before examining GluA1 levels, we checked to see whether neurite outgrowth of NPY-hrGFP neurons could be suppressed in a similar manner as that shown in Fig. 1. The results of exposure to $NaAsO_2$ concentrations of 0, 0.5, 1 and 2 μM showed that neurite elongation was reduced when exposed to the 1 μM concentration and that the reduction became greater at the 2 μM concentration (Fig. 3D-H), indicating that the $NaAsO_2$ concentrations that reduced neurite outgrowth by NPY-hrGFP neurons were the same as those presented in Fig. 1F. Using the same paradigm of $NaAsO_2$ treatment, we measured the immunoflurescent intensity of GluA1 and GluA4 in NPY-hrGFP neurons. The relative intensity of fluorescence using anti-GluA1 antibody was significantly higher in neurons exposed to 0.5 μM $NaAsO_2$ than to other concentrations (Fig. 3I). By contrast, 1 μM $NaAsO_2$ reduced the intensity of the GluA1-immunofluorescent signal and 2 μM $NaAsO_2$ reduced its intensity even more. These results suggested the existence of a relation between the reduction in GluA1 expression level and neurite suppression. On the other hand, the intensity of the GluA4-immunofluorescent signal increased with the concentration of $NaAsO_2$ (Fig. 3J), confirming that $NaAsO_2$ specifically reduces GluA1 expression and does not reduce GluA4 expression. We also investigated the effects of $NaAsO_2$ on GluA2/3 by immunofluorescent

staining with an anti-GluA2/3 antibody, but the immunofluorescent signal for GluA2/3 was weak at DIV4, and there was no marked difference in GluA2/3 immunofluorescent intensity according to whether the cells had been exposed to $NaAsO_2$ or not (data not shown).

3.4 Effects of GluA1 and GluA2 overexpression on impaired neurite outgrowth

To determine whether overexpression of exogenous AMPA receptor subunits could compensate for the decreased GluA1 expression induced by $NaAsO_2$ and rescue the inhibitory effect of $NaAsO_2$ on neurite outgrowth, primary cultured neurons prepared from mouse cerebral cortex were transfected with a plasmid vector to express GFP-fused GluA1 (pGFP-GluA1) or Venus-fused GluA2 (pVenus-GluA2) under the control of a CMV promoter in combination with pmStrawberry and then exposed to 2 μM $NaAsO_2$ from DIV2 to DIV4 (Fig. 4A-D). A pEGFP plasmid vector was used to express GFP was used instead of the GluA1 and GluA2 expression vectors. Neurite outgrowth by the neurons transfected with the control vector expressing GFP was strongly inhibited by 2 μM $NaAsO_2$ (Fig. 4C), whereas neurite outgrowth was stimulated by GluA1 overexpression (Fig. 4B), and its overexpression mitigated the inhibitory effect of $NaAsO_2$ on neurite outgrowth (Fig. 4D). Quantification of total neurite length also demonstrated that 2 μM $NaAsO_2$ significantly reduced the total neurite length of neurites in neurons in the absence of GluA1 overexpression and that the inhibition of neuritogenesis by $NaAsO_2$ was prevented by GluA1 overexpression (Fig. 4E). Exposure to 2 μM $NaAsO_2$ significantly reduced the total number of branches in both the presence and absence of GluA1 overexpression (Fig. 4F). In contrast to its rescuing effect on total neurite length, overexpression of GluA1 did not overcome the significant effect of $NaAsO_2$ on total branch number (Fig. 4F). No significant differences were observed in number of primary branches (Fig. 4G). The numbers of secondary and higher order branches were significantly increased by GluA1 overexpression in the absence of $NaAsO_2$ exposure (Fig. 4H), but their numbers remained low after exposure to $NaAsO_2$ even though GluA1 was overexpressed (Fig. 4H).

GluA2 overexpression had effects on neurite length and the number of branches that were similar to the effects of GluA1 overexpression (Supplementary Fig. S1A-H). The results of GluA2 overexpression are shown in detail in the supplementary text.

4. Discussion

Neuritogenesis in our primary culture of mouse cortical neurons was impaired by exposure to $NaAsO_2$ concentrations of 1 μM or above, and $NaAsO_2$ exposure to the same concentrations also decreased their GluA1 levels. GluA1 overexpression blocked the inhibition of neurite elongation by $NaAsO_2$. These results indicate that the suppression of neurite outgrowth by $NaAsO_2$ may at least be partially attributable to reduced glutamate AMPA receptor expression. On the other hand, exposure to 0.5 μM $NaAsO_2$, a lower concentration than the concentration that induced neurite suppression, increased cell survival and the GluA1 levels according to the immunocytochemistry findings.

4.1 Arsenic-induced suppression of neurite outgrowth and reduction of GluA1 expression

In this study, 1 μM $NaAsO_2$ did not affect cell viability, but strikingly suppressed neurite outgrowth. In a previous study we found that lower concentrations of $NaAsO_2$ affected neuritogenesis before inducing apoptotic and necrotic cell death (Aung et al., 2013). Studies by other groups have shown that neurite damage is a cue for the induction of cell death (Berliocchi et al., 2005, Volbracht et al., 2001). Thus, the suppression of neurite outgrowth may be a primary step in the developmental neurotoxicity of arsenic.

Several hypotheses have been proposed to explain how arsenic suppresses neurite outgrowth. Excitotoxicity is caused by excess levels of neurotransmitters, such as glutamate and other excitatory transmitters, and has been reported to lead to several neurodegenerative diseases (Lau and Tymianski 2010). Since we suspected that excitotoxicity mediates the arsenic-induced neurite suppression, we measured the glutamate concentration in culture medium after $NaAsO_2$ exposure. Surprisingly, the glutamate concentration in the culture medium was unaltered by $NaAsO_2$ (Fig. 2A) and thus excitotoxicity may not be the cause of the neurite suppression in our culture system. A decrease in the number of glutamate receptor(s) is another possible cause of neurodegenerative diseases, because changes in cerebral AMPA receptor expression have been reported in neurodegenerative diseases (Optiz et al., 2000), and AMPA receptor knockdown itself is a cause and an aggravating factor of neurodegeneration (Oguro et al., 1999). We performed two experiments to test the hypothesis that $NaAsO_2$ suppresses AMPA receptor expression. In the first experiment, AMPA receptor protein levels in total cell lysates were measured by immunoblot. The results showed that $NaAsO_2$ at concentrations of 1 μM and above reduced the GluA1 levels and that the reductions paralleled the suppression of neurite elongation. In the second experiment, we performed immunocytochemistry on NPY-hrGFP neurons to verify the result of the first

experiment. NPY neurons localized mainly in layer II/III and VI of the cerebral cortex (van den Pol et al., 2009) are known to be involved in neurological diseases such as epilepsy, schizophrenia, depression and ADHD (Lesch et al., 2011; Brothers and Wahlestedt, 2010; Connor et al., 2011). NPY neurons have been reported to function as inhibitory interneurons (Gelman et al., 2011). NPY-hrGFP neurons have a great advantage of allow examination of the detailed morphology of NPY neurons through green fluorescence without specific staining. Since neurites of NPY-hrGFP neurons were as vulnerable to $NaAsO_2$ as the neurites of neurons transfected with pmStrawberry (Fig. 3D-H), we concluded that NPY-hrGFP neurons could be used as a typical example of cortical neurons in regard to sensitivity to $NaAsO_2$. It is also advantageous to utilize NPY-hrGFP neurons when evaluating GluA1 levels, because most NPY-hrGFP neurons exhibited GluA1-immunoreactivity in our culture system (Fig.3C). The immunocytochemistry analysis of GluA1 in NPY-hrGFP neurons confirmed that $NaAsO_2$ at concentrations of 1 μM and above reduced GluA1 expression. Based on the consistent results obtained in these two experiments, we speculated that reduced GluA1 expression is a factor that links $NaAsO_2$ exposure to impaired neurite outgrowth. Since exposing rats to arsenic has been reported to increase the glutamate content of their brain (Nagaraja and Desiraju, 1993), the possibility remains that excitotoxicity still occurs following arsenic exposure in *in vivo*. Further study will be necessary to determine whether arsenic affects glutamate release and/or glutamate AMPA receptor expression *in vivo*.

Some etiological causes explaining how $NaAsO_2$ reduces GluA1 levels can be proposed. Arsenic is known to induce oxidative stress, and oxidative stress leads to the suppression of neurite outgrowth and changes in cytoskeletal proteins expression (DeFuria and Shea, 2007; Wang et al., 2010). We recently demonstrated that $NaAsO_2$ specifically changed the gene expression of cytoskeletal proteins in Neuro2A cells (Aung et al., 2013). Exposure to $NaAsO_2$ dose-dependently reduced the mRNA levels of tau and tubulin in Neuro2A cells but increased the mRNA levels of the light and medium subunits of neurofilaments. Since the intracellular transport, synaptic insertion and recycling of GluA1 have been reported to be controlled by cytoskeletal proteins (Anggono and Huganir, 2012; Perestenko and Henley, 2003), reduced GluA1 levels may be caused by cytoskeletal dysfunction in response to oxidative stress induced by $NaAsO_2$. Apart from cytoskeletal dysfunction, epigenetic regulation of GluA1 may be responsible for the arsenic-induced suppression of neurite outgrowth. It has been reported that expression of HDAC2, a subtype of histone deacetylase sensitive to neurotoxic insults, was found to increase in response to oxidative stress and neurotoxic accumulation of β-amyloid, and that the increase reduced gene expression of proteins related to synaptic plasticity including GluA1, as a result of deacetylation

of histones localized at their promoters (Gräff et al. 2012). Given that arsenic affects HDAC2 expression through eliciting oxidative stress, GluA1 expression may be reduced by the activity of HDAC2. These hypotheses should be tested in future studies.

4.2 Rescue from arsenic-induced suppression of neurite outgrowth by overexpression of GluA

Compensatory overexpression of GluA1 partially reversed the neurite suppression induced by 2 μM $NaAsO_2$ in this study (Fig. 4), thereby indicating that the impaired neurite outgrowth is at least partly due to the reduction of the GluA1 expression level. AMPA receptors composed of any tetrameric combination of GluA1-4 subunits are permeable to Na^+ after glutamate binds to them, whereas Ca^{2+} permeability depends on their subunit composition. AMPA receptors lacking GluA2 are Ca^{2+}-permeable, whereas AMPA receptors containing GluA2 are Ca^{2+}-impermeable (Hume et al., 1991; Verdoorn et al., 1991). Since overexpression of GluA1 and GluA2 has been reported to increase total neurite length by increasing neuronal excitability (Prithviraj et al., 2008, Chen et al., 2009), both GluA1 and GluA2 may be associated with neuritogenesis despite the difference in Ca^{2+} permeability. In our case, overexpression of GluA2 as well as GluA1 partly reversed the impaired neurite outgrowth (Fig.4 and Supplementary Fig. 1). Therefore, the recovery from impaired neurite outgrowth caused by $NaAsO_2$ is likely to be related to the increase in neuronal excitability as a result of Na^+ entry rather than due to Ca^{2+} entry.

The observation that GluA overexpression rescues neurons from arsenic neurotoxicity implies that GluA stimulation by certain drugs may have a therapeutic effect on neurodegeneration induced by arsenic. AMPA receptor agonists and modulators, such as ampakines, might be candidate drugs for the prevention and/or treatment of arsenic-induced neurodegeneration.

4.3 Effect of low arsenic concentrations on neurons

Although exposure to $NaAsO_2$ concentrations of 1 μM and above reduced cell survival, the 0.5 μM concentration of $NaAsO_2$ had the opposite effect and at rather significantly increased cell survival, and immunocytochemistry measurements showed that it tended to increase neurite outgrowth and significantly increased GluA1 levels when measured by immunocytochemistry. Exposure to arsenic concentrations below the concentration that causes cell death has been reported to stimulate keratinocyte proliferation and vascular cell proliferation through overexpression of growth factors and activation of tyrosine phosphorylation, respectively (Germolec et al., 1996; Barchowsky et al., 1999). We have not yet identified the pathway by

which arsenic increases cell survival and GluA1 levels in neurons at concentrations below the concentration that suppresses neurite growth. It should be identified in a future study.

The occurrence of neurodevelopmental disorders such as autism and ADHD have been suspected of being associated with exposure to environmental chemicals, including arsenic (Grandjean et al., 2006). Increases in the size of some brain regions and decreases in the size of others have been reported in neurodevelopmental disease (Seidman et al. 2011; Bauman and Kemper, 2005), and these anomalies might be responsible for patient's cognitive dysfunction. If arsenic affects the brain differently depending on its concentration, since great differences in arsenic distribution among brain regions have been reported after exposure to arsenic, reduction and stimulation of cell survival and/or neurite outgrowth may occur simultaneously in different brain regions (Sánchez-Peña et al., 2010). Therefore, not only a decrease but also an increase in cell number and/or neurite outgrowth might be taken into account as a feature of arsenic adverse effects. The hypothesis that arsenic exerts its toxic effects through mechanisms that differ according to the brain regions will need to be tested in experimental animals in the future.

5. Conclusions

In conclusion, exposure to arsenic at concentrations below the concentration that caused cell death in primary cultures of cortical neurons impaired neuritogenesis and we speculate that impaired neuritogenesis is partly due to reduction of GluA1 expression. By contrast, cell survival and GluA1 expression both increased when exposed to $NaAsO_2$ concentrations below the concentrations that impaired neurite outgrowth. Future studies will be required to determine whether these findings in culture systems also occur in experimental animals *in vivo*.

Acknowledgement

The authors gratefully thank Drs. Masami Ishido, Junko Suzuki and Daisuke Nakajima (NIES) for their kind helps on use of confocal microscope and Mr. Yuichi Akiyama (Keyence) for his help on use of BZ-8000 microscope. We also thank Dr. Atsushi Miyawaki (Riken Brain Science Institute, Japan) for providing pmStrawberry and pVenus and Prof. Jeremy M. Henley (University of Bristol, United Kingdom) for providing pEGFP-GluR1. We also thank Ms. Hikari Murai and Michiyo Matsumoto for their superior technical assistance and Ms. Sayuri Itaki for her excellent secretarial assistance. The authors also thank staff of Animal Care Company (Tokyo, Japan) for their excellent assistance in the maintenance of wild-type and transgenic mice.

Author Contributions

Conceived and designed the experiments: FM and KN. Performed the experiments: FM. Analyzed the data: FM, TT, KA, ST, KN. Contributed reagents/materials/analysis tools: TT, KA, ST, LP, KN. Wrote the paper: FM.

Funding

This work was supported by the National Institute for Environmental Studies [0710AG333, 115AA082], by the Ministry of the Environment [Environment Research and Technology Development Fund, S-01], by KAKENHI [22790228, 23310043, 23390166, 24590307], and by a grant from the Japan Chemical Industry Association (JCIA) Long-range Research Initiative (LRI).

Competing interests

The authors have declared that no competing interests exist.

References

Anggono V, Huganir RL. Regulation of AMPA receptor trafficking and synaptic plasticity. Curr Opin Neurobiol. 2012; 22:461-9.

Aung K, Kurihara R, Nakashima S, Maekawa F, Nohara K, Kobayashi T, Tsukahara S. Inhibition of neurite outgrowth and alteration of cytoskeletal gene expression by sodium arsenite. Neurotoxicology 2013; 34:226-35.

Barchowsky A, Roussel RR, Klei LR, James PE, Ganju N, Smith KR, Dudek EJ. Low levels of arsenic trioxide stimulate proliferative signals in primary vascular cells without activating stress effector pathways. Toxicol Appl Pharmacol. 1999; 159:65-75.

Bauman ML, Kemper TL. Neuroanatomic observations of the brain in autism: a review and future directions. Int J Dev Neurosci. 2005; 23:183-7.

Berliocchi L, Fava E, Leist M, Harvat V, Dinsdale D, Read D, et al. Botulinum neurotoxin C initiates two different programs for neurite degeneration and neuronal apoptosis. J Cell Biol 2005; 168:607–18.

Brothers SP, Wahlestedt C. Therapeutic potential of neuropeptide Y (NPY) receptor ligands. EMBO Mol Med. 2010; 2:429-39.

Calderón J, Navarro ME, Jimenez-Capdeville ME, Santos-Diaz MA, Golden A, Rodriguez-Leyva I, Borja-Aburto V, Díaz-Barriga F. Exposure to arsenic and lead and neuropsychological development in Mexican children. Environ Res. 2001;85:69-76.

Chen W, Prithviraj R, Mahnke AH, McGloin KE, Tan JW, Gooch AK, Inglis FM.AMPA glutamate receptor subunits 1 and 2 regulate dendrite complexity and spine motility in neurons of the developing neocortex. Neuroscience. 2009; 159:172-82.

Chenal J, Pellerin L. Noradrenaline enhances the expression of the neuronal monocarboxylate transporter MCT2 by translational activation via stimulation of PI3K/Akt and the mTOR/S6K pathway. J Neurochem. 2007; 102 :389-97.

Connor CM, Crawford BC, Akbarian S. White matter neuron alterations in schizophrenia and related disorders. Int J Dev Neurosci. 2011; 29:325-34.

Costa LG, Aschner M, Vitalone A, Syversen T, Soldin OP. Developmental neuropathology of environmental agents. Annu Rev Pharmacol Toxicol 2004;44:87−110.

Dakeishi M, Murata K, Grandjean P. Long-term consequences of arsenic poisoning during infancy due to contaminated milk powder. Environ Health. 2006; 5:31.

DeFuria J, Shea TB. Arsenic inhibits neurofilament transport and induces perikaryal accumulation of phosphorylated neurofilaments: roles of JNK and GSK-3beta. Brain Res. 2007 ;1181:74-82.

Farina M, Rocha JB, Aschner M. Mechanisms of methylmercury-induced neurotoxicity: evidence from experimental studies. Life Sci. 2011; 89:555-63.

Frankel S, Concannon J, Brusky K, Pietrowicz E, Giorgianni S, Thompson WD, et al. Arsenic exposure disrupts neurite growth and complexity in vitro. Neurotoxicology 2009; 30:529-37.

Gelman D, Griveau A, Dehorter N, Teissier A, Varela C, Pla R, Pierani A, Marín O. A wide diversity of cortical GABAergic interneurons derives from the embryonic preoptic area. J Neurosci. 2011; 31:16570-80.

Germolec DR, Yoshida T, Gaido K, Wilmer JL, Simeonova PP, Kayama F, Burleson F, Dong W, Lange RW, Luster MI. Arsenic induces overexpression of growth factors in human keratinocytes. Toxicol Appl Pharmacol. 1996; 141:308-18.

González-Albo MC, Elston GN, DeFelipe J. The human temporal cortex: characterization of neurons expressing nitric oxide synthase, neuropeptides and calcium-binding proteins, and their glutamate receptor subunit profiles. Cereb Cortex. 2001; 11:1170-81.

Goulet S, Doré FY, Mirault ME. Neurobehavioral changes in mice chronically exposed to methylmercury during fetal and early postnatal development. Neurotoxicol Teratol 2003; 25:335-47.

Gräff J, Rei D, Guan JS, Wang WY, Seo J, Hennig KM, Nieland TJ, Fass DM, Kao PF, Kahn M,

Su SC, Samiei A, Joseph N, Haggarty SJ, Delalle I, Tsai LH. An epigenetic blockade of cognitive functions in the neurodegenerating brain. Nature. 2012; 483:222-6.

Grandjean P, Landrigan PJ. Developmental neurotoxicity of industrial chemicals. Lancet 2006; 368:2167-78.

Hamadani JD, Tofail F, Nermell B, Gardner R, Shiraji S, Bottai M, et al. Critical windows of exposure for arsenic-associated impairment of cognitive function in pre-school girls and boys: a population-based cohort study. Int J Epidemiol 2011; 40:1593-604.

Hume RI, Dingledine R, Heinemann SF. Identification of a site in glutamate receptor subunits that controls calcium permeability. Science. 1991; 253:1028-31.

Kawaguchi Y, Kubota Y. GABAergic cell subtypes and their synaptic connections in rat frontal cortex. Cereb Cortex. 1997; 7:476-86.

Koike-Kuroda Y, Kakeyama M, Fujimaki H, Tsukahara S. Use of live imaging analysis for evaluation of cytotoxic chemicals that induce apoptotic cell death. Toxicol In Vitro 2010; 24:2012-20.

Kumar J, Mayer ML. Functional Insights from Glutamate Receptor Ion Channel Structures. Annu Rev Physiol. 2012 [Epub ahead of print].

Lau A, Tymianski M. Glutamate receptors, neurotoxicity and neurodegeneration. Pflugers Arch. 2010 ;460:525-42.

Lesch KP, Selch S, Renner TJ, Jacob C, Nguyen TT, Hahn T, Romanos M, Walitza S, Shoichet S, Dempfle A, Heine M, Boreatti-Hümmer A, Romanos J, Gross-Lesch S, Zerlaut H, Wultsch T, Heinzel S, Fassnacht M, Fallgatter A, Allolio B, Schäfer H, Warnke A, Reif A, Ropers HH, Ullmann R. Genome-wide copy number variation analysis in attention-deficit/hyperactivity disorder: association with neuropeptide Y gene dosage in an extended pedigree. Mol Psychiatry. 2011; 16:491-503.

Maekawa F, Tsuboi T, Fukuda M, Pellerin L. Regulation of the intracellular distribution, cell surface expression, and protein levels of AMPA receptor GluR2 subunits by the

monocarboxylate transporter MCT2 in neuronal cells. J Neurochem. 2009; 109: 1767-78.

Martinez EJ, Kolb BL, Bell A, Savage DD, Allan AM. Moderate perinatal arsenic exposure alters neuroendocrine markers associated with depression and increases depressive-like behaviors in adult mouse offspring. Neurotoxicology. 2008; 29:647-55.

Martinez-Finley EJ, Ali AM, Allan AM. Learning deficits in C57BL/6J mice following perinatal arsenic exposure: consequence of lower corticosterone receptor levels? Pharmacol Biochem Behav. 2009; 94:271-7.

Meijering E, Jacob M, Sarria JC, Steiner P, Hirling H, Unser M. Design and validation of a tool for neurite tracing and analysis in fluorescence microscopy images. Cytometry A. 2004;58 :167-76.

Nagaraja TN, Desiraju T. Regional alterations in the levels of brain biogenic amines, glutamate, GABA, and GAD activity due to chronic consumption of inorganic arsenic in developing and adult rats. Bull Environ Contam Toxicol. 1993;50:100-7.

Oguro K, Oguro N, Kojima T, Grooms SY, Calderone A, Zheng X, Bennett MV, Zukin RS. Knockdown of AMPA receptor GluR2 expression causes delayed neurodegeneration and increases damage by sublethal ischemia in hippocampal CA1 and CA3 neurons. J Neurosci. 1999; 19:9218-27.

Opitz T, Grooms SY, Bennett MV, Zukin RS. Remodeling of alpha-amino-3-hydroxy-5-methyl-4-isoxazole-propionic acid receptor subunit composition in hippocampal neurons after global ischemia. Proc Natl Acad Sci U S A. 2000; 97:13360-5.

Perestenko PV, Henley JM. Characterization of the intracellular transport of GluR1 and GluR2 alpha-amino-3-hydroxy-5-methyl-4-isoxazole propionic acid receptor subunits in hippocampal neurons. J Biol Chem. 2003; 278:43525-32.

Prithviraj R, Kelly KM, Espinoza-Lewis R, Hexom T, Clark AB, Inglis FM. Differential regulation of dendrite complexity by AMPA receptor subunits GluR1 and GluR2 in motor neurons. Dev Neurobiol. 2008; 68:247-64.

Ríos R, Zarazúa S, Santoyo ME, Sepúlveda-Saavedra J, Romero-Díaz V, Jiménez V, Pérez-Severiano F, Vidal-Cantú G, Delgado JM, Jiménez-Capdeville ME. Decreased nitric oxide markers and morphological changes in the brain of arsenic-exposed rats. Toxicology. 2009; 261:68-75.

Rodríguez VM, Carrizales L, Mendoza MS, Fajardo OR, Giordano M. Effects of sodium arsenite exposure on development and behavior in the rat. Neurotoxicol Teratol. 2002; 24:743-50.

Sánchez-Peña LC, Petrosyan P, Morales M, González NB, Gutiérrez-Ospina G, Del Razo LM, Gonsebatt ME. Arsenic species, AS3MT amount, and AS3MT gene expression in different brain regions of mouse exposed to arsenite. Environ Res. 2010; 110:428-34.

Seidman LJ, Biederman J, Liang L, Valera EM, Monuteaux MC, Brown A, Kaiser J, Spencer T, Faraone SV, Makris N. Gray matter alterations in adults with attention-deficit/hyperactivity disorder identified by voxel based morphometry. Biol Psychiatry. 2011; 69:857-66.

Tsai SY, Chou HY, The HW, Chen CM, Chen CJ. The effects of chronic arsenic exposure from drinking water on the neurobehavioral development in adolescence. Neurotoxicology. 2003; 24:747-53.

van den Pol AN, Yao Y, Fu LY, Foo K, Huang H, Coppari R, Lowell BB, Broberger C. Neuromedin B and gastrin-releasing peptide excite arcuate nucleus neuropeptide Y neurons in a novel transgenic mouse expressing strong Renilla green fluorescent protein in NPY neurons. J Neurosci. 2009; 29:4622-39.

Verdoorn TA, Burnashev N, Monyer H, Seeburg PH, Sakmann B. Structural determinants of ion flow through recombinant glutamate receptor channels. Science. 1991; 252:1715-8.

Voss OP, Milne S, Sharkey J, O'Neill MJ, McCulloch J. Molecular mechanisms of neurite growth with AMPA receptor potentiation. Neuropharmacology. 2007; 52:590-7.

Volbracht C, Leist M, Kolb SA, Nicotera P. Apoptosis in caspase-inhibited neurons. Mol Med 2001; 7:36–48.

Wang SX, Wang ZH, Cheng XT, Li J, Sang ZP, Zhang XD, et al. Arsenic and fluoride exposure in

drinking water: children's IQ and growth in Shanyin country, Shanxi province, China. Environ Health Prospect 2007; 115:643-7.

Wang X, Meng D, Chang Q, Pan J, Zhang Z, Chen G, et al. Arsenic inhibits neurite outgrowth by inhibiting the LKB1-AMPK signaling pathway. Environ Health Perspect 2010; 118:627-34.

Wasserman GA, Liu X, Parvez F, Ahsan H, Factor-Litvak P, Kline J, et al. Water arsenic exposure and intellectual function in 6-year-old children in Araihazar, Bangladesh. Environ Health Perspect 2007; 115:285-9.

Wasserman GA, Liu X, Parvez F, Ahsan H, Factor-Litvak P, Kline J, et al. Water arsenic exposure and children's intellectual function in Araihazar, Bangaladesh. Environ Health Perspect 2004; 112:1329-33.

Winneke G. Developmental aspects of environmental neurotoxicology: lessons from lead and polychlorinated biphenyls. J Neurol Sci 2011; 308:9-15.

Xi S, Sun W, Wang F, Jin Y, Sun G. Transplacental and early life exposure to inorganic arsenic affected development and behavior in offspring rats. Arch Toxicol. 2009; 83: 549-56.

Figure Legends

Fig. 1. Effects of $NaAsO_2$ on cell viability and neurite outgrowth in primary cultures of neurons. A. Cell viability was assessed using the WST-1 assay. Cell viability was significantly reduced by exposure to 2 μM $NaAsO_2$ (b, $p<0.01$ vs 0, 0.125, 0.25, 0.5, 1 μM). No significant decrease of cell viability was found between the exposures to 0 μM and 1 μM $NaAsO_2$. The exposure to 0.5 μM $NaAsO_2$ rather increased cell viability when compared to 0, 1 and 2 μM (a, $p<0.01$). **B-E.** Confocal images of neurons exposed to 0, 0.5, 1 and 2 μM $NaAsO_2$ from DIV2 to 4. **F.** Total neurite length of neurons exposed to 0, 0.5, 1 and 2 μM $NaAsO_2$ from DIV2 to 4. A significant reduction of total neurite length per cell was found at 1 μM (a, $p<0.05$ vs 0 μM and $p<0.01$ vs 0.5 μM) and the degree of reduction was more severe at 2 μM (b, $p<0.01$ vs 0 and 0.5 μM). **G.** Total number of branches. **H.** Number of primary branches. **I.** The number of secondary and higher order branches. The number of secondary and higher order branches was significantly decreased in groups exposed to 1 μM or 2 μM $NaAsO_2$ when compared to the group exposed to 0.5 μM $NaAsO_2$ (a, $p<0.01$ vs 1.0 and 2.0 μM), but there was no significant difference when compared to the group at 0 μM.

Fig. 2. Effects of $NaAsO_2$ on extracellular glutamate levels and expression of AMPA receptors. A. The concentration of glutamate in the culture medium of primary neurons had been exposed to $NaAsO_2$ at concentrations of 0, 0.125, 0.25, 0.5, and 1 μM from DIV2 to DIV4. There was no difference in the concentrations of glutamate among groups. **B.** Immunoblot analyses of GluA1 and control β-actin expression levels. **C.** Quantification of optical density (O.D.) of bands revealed that GluA1 expression was significantly decreased by the exposure to 1 μM $NaAsO_2$ (a, $p<0.01$ vs 0 μM and $p<0.05$ vs 0.5 μM) and the decrease became more severe by the exposure to 2 μM $NaAsO_2$ (b, $p<0.01$ vs 0 and 0.5 μM and $p<0.05$ vs 1.0 μM). **D.** Immunoblot analyses of AMPA receptors GluA1, 2/3 and 4 at the concentrations of 0 and 1 μM $NaAsO_2$. MAP2 and β-actin were used as controls. **E.** GluA1 levels were significantly decreased by the exposure to 1 μM $NaAsO_2$ (a, $p<0.01$ vs 0 μM). GluA2/3 and GluA4 levels were unchanged.

Fig. 3. Effect of $NaAsO_2$ on GluA1 expression in primary-cultured NPY-hrGFP neurons. A. Macroscopic view of the cerebral cortex emitting green fluorescence from the transgenic mouse expressing a humanized Renilla green fluorescence protein (hrGFP) under the regulation of the neuropeptide Y (NPY) gene promoter (NPY-hrGFP). **B.** Immunocytochemistry of GluA1 in NPY-hrGFP neurons. Green indicates hrGFP-tagged NPY neuron. Red indicates

GluA1-immunoreactivity. Blue indicates 4',6-diamidino-2-phenylindole (DAPI) which reflects the nuclei. Arrows indicate the NPY-hrGFP and GluA1-double positive cells and arrowheads indicate GluA1-single positive cells. Most of NPY-hrGFP neurons shown here exhibited GluA1-immunoreactivity. C. Percentage of GluA1-positive neurons compared to total NPY-hrGFP neuron. 98.5% of NPY-hrGFP neurons were GluA1-positive D-G. Morphology of NPY-hrGFP neurons exposed to $NaAsO_2$ at concentrations of 0, 0.5, 1 and 2 μM. H. Total neurite length of NPY-hrGFP neurons exposed to 0, 0.5, 1 and 2 μM $NaAsO_2$ from DIV2 to DIV4. The length of neurites was significantly decreased at the exposure to 1 μM $NaAsO_2$ (a, $p<0.01$ vs 1 and 2 μM; b, $p<0.05$ vs 0 and 2 μM ; c, $p< 0.01$ vs 0 μM) and the decrease became more severe at 2 μM $NaAsO_2$. I. Effect of $NaAsO_2$ on relative intensity of GluA1 immunoreactivity in NPY-hrGFP neuron. Relative intensity became significantly higher by the exposure to 0.5 μM $NaAsO_2$ (a, $p<0.01$ vs 0, 1 and 2 μM). By contrast, the exposure to 1 μM $NaAsO_2$ significantly reduced the relative intensity (b, $p<0.01$ vs 0 and 2 μM; c, $p<0.01$ vs 0 μM) and the exposure to 2 μM $NaAsO_2$ induced more important reduction. J. Effect of $NaAsO_2$ on the relative intensity of GluA4 immunoreactivity in NPY-hrGFP neurons. Relative intensity of GluA4 immunoreactivity rather increased with the concentrations of $NaAsO_2$ (a, $p<0.01$ vs 0 and 2 μM, $p<0.05$ vs 1 μM; b, $p<0.01$ vs 0 μM, $p<0.05$ vs 2 μM; c, $p<0.01$ vs 0 μM).

Fig. 4. Effects of GluA1 overexpression on impaired neurite outgrowth induced by $NaAsO_2$

A-D. Effect of the combination of GluA1 overexpression and $NaAsO_2$ treatment on neurite outgrowth. "$NaAsO_2$(+)" indicates the exposure to 2 μM $NaAsO_2$ from DIV2 to DIV4 and "$NaAsO_2$(-)" indicates no such exposure. "GluA1(+)" indicates neurons transfected with pGFP-GluA1 and "GluA1(-)" indicates neurons transfected with control pEGFP. E. Changes in total neurite length induced by the combination of GluA1 overexpression and $NaAsO_2$ treatment. GluA1 overexpression significantly increased total neurite length of neurons with no $NaAsO_2$ treatment (a, $p<0.01$ vs other groups). The exposure to $NaAsO_2$ significantly reduced total neurite length (b, $p<0.05$ vs $NaAsO_2$(-)-GluA1(-) group) but GluA1 overexpression alleviated the inhibitory effects of $NaAsO_2$ on neurite length (c, $p<0.01$ vs NaAsO2(-)-GluA1(+) and NaAsO2(+)-GluA1(-) groups). F. Total number of neurite branches. The treatment with $NaAsO_2$ significantly reduced the total number of branches and GluA1 overexpression tended to increase the total number of branches but the overexpression could not overcome the effect of $NaAsO_2$ (a, $p<0.01$ vs $NaAsO_2$ (+)-GluA1(-) group, $p<0.05$ vs $NaAsO_2$ (+)GluA1(+) group; b, $p<0.05$ vs $NaAsO_2$(-)-GluA1(-) group). G. The number of primary branches. No difference was found

among groups. H. The number of secondary and higher order branches. GluA1 overexpression increased the number in $NaAsO_2$-untreated groups (a, $p<0.01$ vs other groups) but it could not overcome the effect of $NaAsO_2$ treatment.

Figures

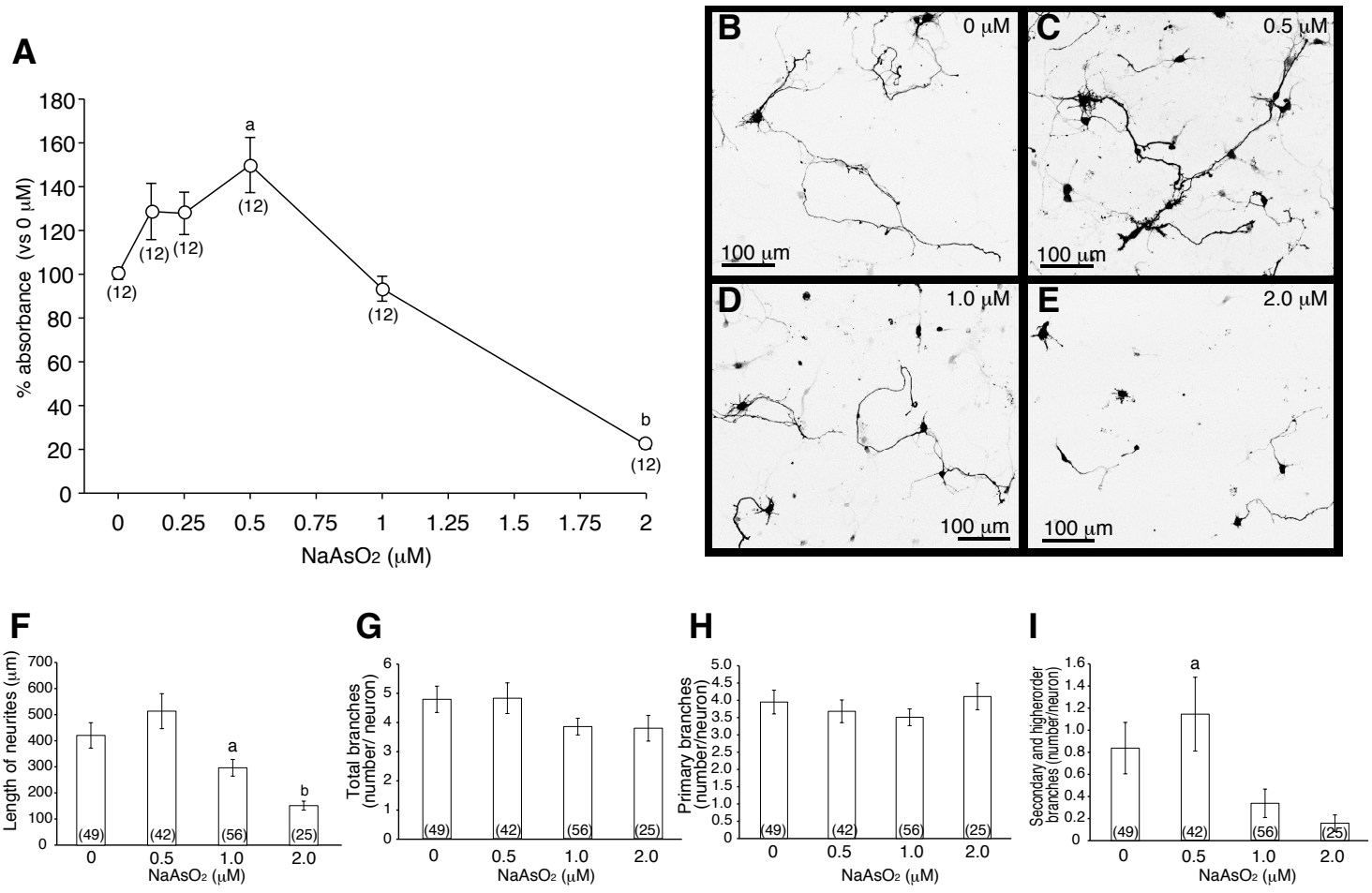

Fig. 1

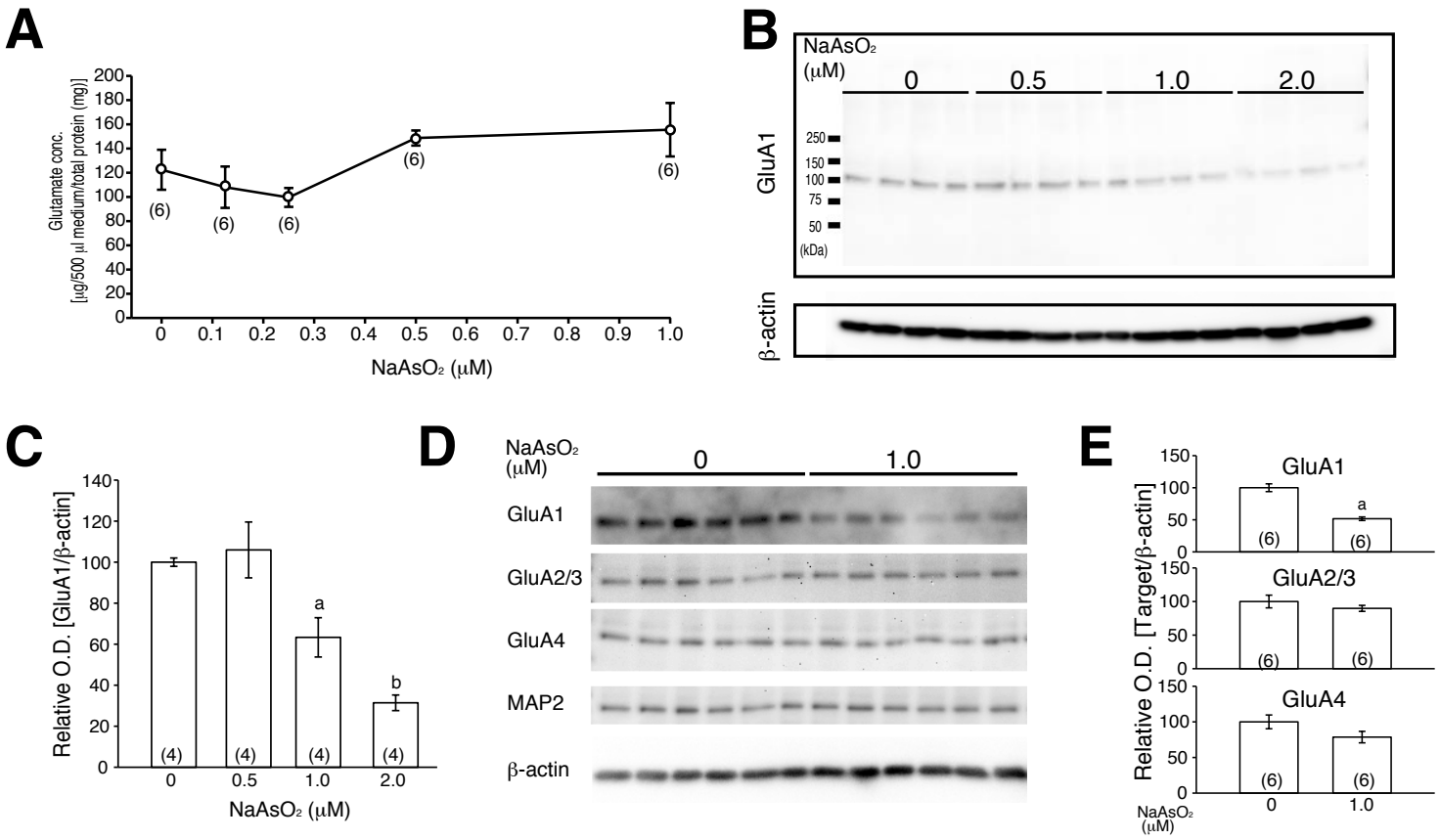
A
Glutamate conc.
[μg/500 μl medium/total protein (mg)]
NaAsO₂ (μM)
(6)
B
NaAsO₂
(μM)
0
0.5
1.0
2.0
GluA1
β-actin
(kDa)
C
Relative O.D. [GluA1/β-actin]
NaAsO₂ (μM)
a
b
(4)
D
NaAsO₂
(μM)
GluA1
GluA2/3
GluA4
MAP2
β-actin
E
GluA1
GluA2/3
GluA4
Relative O.D. [Target/β-actin]
NaAsO₂
(μM)

Fig. 2

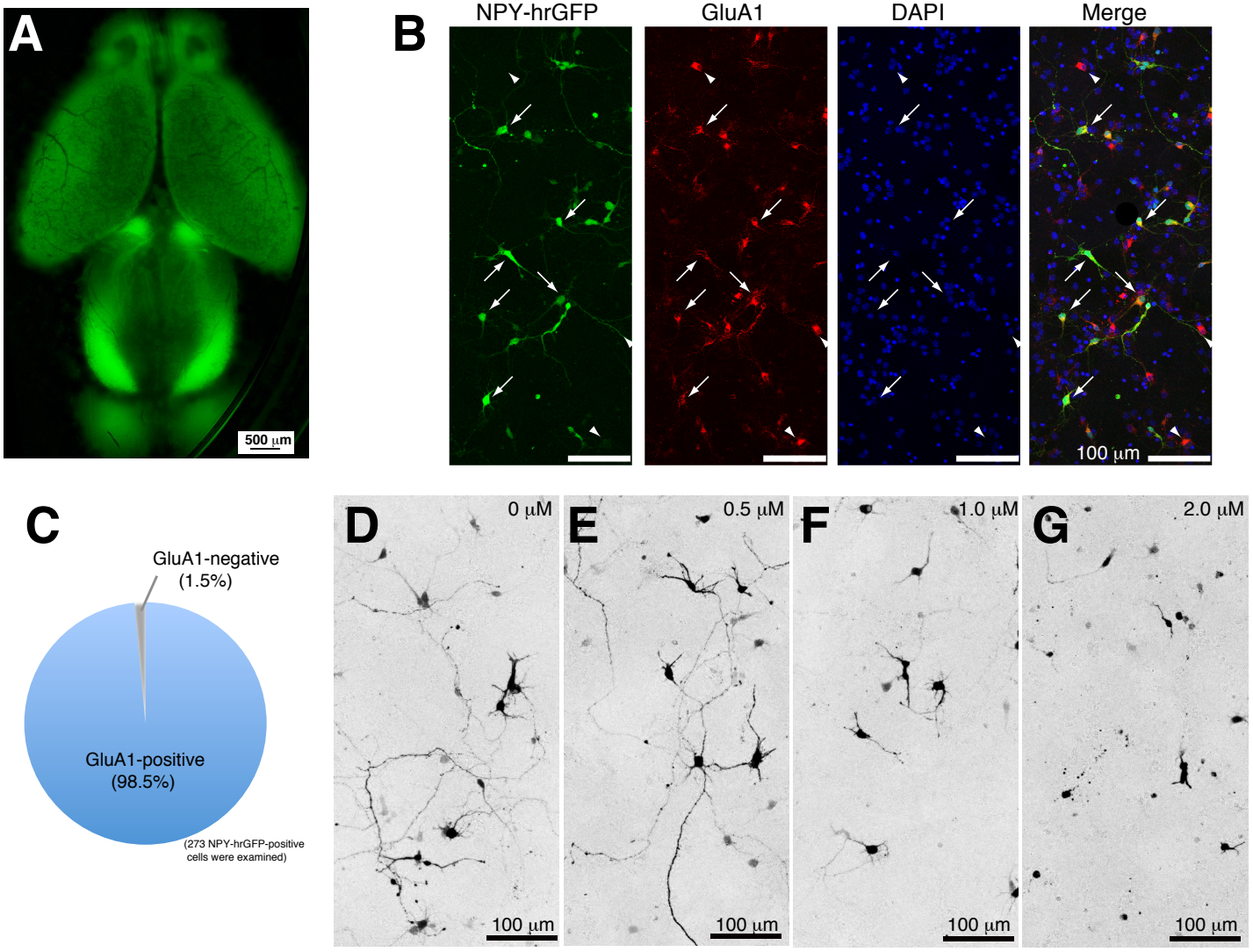
A
500 μm
B
NPY-hrGFP
GluA1
DAPI
Merge
100 μm
C
GluA1-negative
(1.5%)
GluA1-positive
(98.5%)
(273 NPY-hrGFP-positive
cells were examined)
D
0 μM
E
0.5 μM
F
1.0 μM
G
2.0 μM
100 μm
H
Length of neurites (μm)
NaAsO2 (μM)
I
Relative intensity
NaAsO2 (μM)
J
Relative intensity
NaAsO2 (μM)

Fig. 3

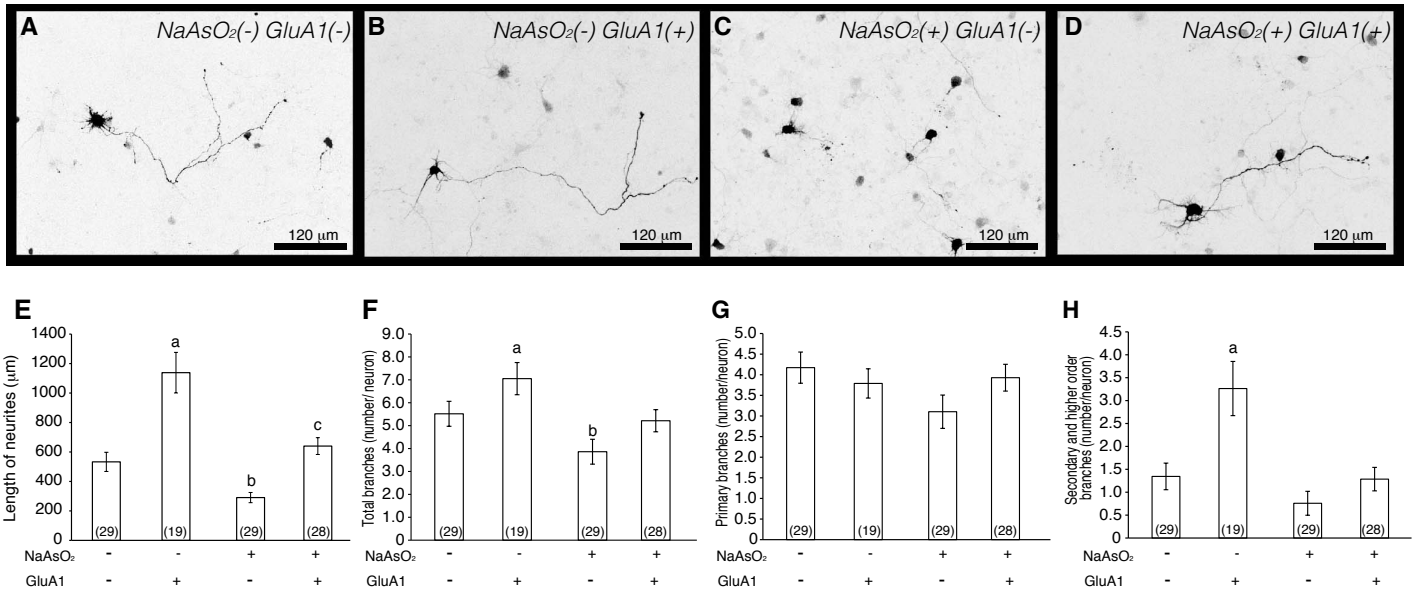
A
NaAsO2(-) GluA1(-)
120 μm
B
NaAsO2(-) GluA1(+)
120 μm
C
NaAsO2(+) GluA1(-)
120 μm
D
NaAsO2(+) GluA1(+)
120 μm
E
Length of neurites (μm)
1400
1200
1000
800
600
400
200
0
a
b
c
(29)
(19)
(29)
(28)
NaAsO2 - - + +
GluA1 - + - +
F
Total branches (number/ neuron)
9.0
8.0
7.0
6.0
5.0
4.0
3.0
2.0
1.0
0
a
b
(29)
(19)
(29)
(28)
NaAsO2 - - + +
GluA1 - + - +
G
Primary branches (number/neuron)
5.0
4.5
4.0
3.5
3.0
2.5
2.0
1.5
1.0
0.5
0
(29)
(19)
(29)
(28)
NaAsO2 - - + +
GluA1 - + - +
H
Secondary and higher order branches (number/neuron)
4.5
4.0
3.5
3.0
2.5
2.0
1.5
1.0
0.5
0
a
(29)
(19)
(29)
(28)
NaAsO2 - - + +
GluA1 - + - +

Fig. 4